Electronic Supplementary Material (ESI) for Journal of Materials Chemistry C.

Supplementary Information

Lewis Acid-Base Pair Doping of *p*-Type Organic Semiconductors

Kelly A. Peterson,[a] Michael L. Chabinyc[a]

[a] *Materials Department, University of California, Santa Barbara, California 93106, USA*

Contents

Experimental Methods

Materials

Except where noted, dry $B(C_6F_5)_3$ (98%, TCI America, used as received, stored at room temperature in N_2 glovebox) was used for all experiments. Benzoyl peroxide (Luperox A98) was used as received within 6-8 months of opening the bottle. Decamethylferrocene (97%, Sigma Aldrich) was used as received.

Purchased polymers were used as received: P3HT (Merck Lisicon SP001), RRa-P3HT (Sigma Aldrich), MEH-PPV (LumTec), and PFO (ADS). C_2C_6-IDTBT was synthesized by the McCulloch Lab as previously described.[1] Anhydrous solvents were used as received: chloroform (anhydrous, Sigma Aldrich); chlorobenzene (anhydrous, 99.8%, Sigma Aldrich); dichloromethane (anhydrous, ≥99.8%, 40-150 ppm amylene, Sigma Aldrich); pentane (anhydrous, 99+%, Sigma Aldrich); acetonitrile (99.9% Extra Dry, Acros Organics).

Anhydrous CD_2Cl_2 was prepared by drying CD_2Cl_2 (0.03% v/v TMS, Sigma Aldrich) with 4 Å molecular sieves (8-12 mesh, Fisher) for at least 3 days in a N_2 glovebox. Molecular sieves were dried for 24 h under vacuum in a vacuum oven at 150-200 °C. Anhydrous $CDCl_3$ was prepared by degassing $CDCl_3$ (Cambridge Isotope Laboratories) then drying with 4 Å molecular sieves as described above.

Spectroscopic Characterization

P3HT solutions for UV-Vis were prepared by first dissolving P3HT at 1 mg/mL, BCF at 6.2 mg/mL, and BPO at 1.5 mg/mL in chloroform. We added chloroform, BCF solution, BPO solution (in that order) to the P3HT solutions in the desired ratios so that the doped solution is at a P3HT concentration of 0.5 mg/mL. Doped solutions were stirred at room temperature at 300 rpm for 1-3 hours. Then, 50 µL of doped solution was diluted with 2 mL of chloroform in a capped 1 cm quartz cuvette for measurement. UV-Vis spectra were taken on a Shimadzu UV-3600 or UV-2600 spectrometer. Solutions of RRa-P3HT were prepared in a similar manner with DCM as the solvent. RRa-P3HT was dissolved at 0.5 mg/mL in DCM, doped at 0.33 mg/mL of RRa-P3HT, and diluted to 0.012 mg/mL of RRa-P3HT for UV-Vis measurement.

Solutions of the other polymers were prepared in a similar manner, except using air-exposed BCF (95%, Sigma Aldrich, see NMR below) and using chlorobenzene as the solvent. MEH-PPV was initially dissolved at 5 mg/mL in chlorobenzene, doped at 2.34 mg/mL of MEH-PPV, and diluted to 0.017 mg/mL of MEH-PPV for UV-Vis measurement. IDTBT was dissolved at 5 mg/mL in chlorobenzene, doped at 3 mg/mL of IDTBT, and diluted to 0.02 mg/mL of IDTBT for UV-Vis measurement. PFO was dissolved at 5 mg/mL in chlorobenzene, doped at 2.5 mg/mL of PFO, and diluted to 0.017 mg/mL of PFO for UV-Vis measurement.

UV-Vis-NIR spectra were recorded on a Shimadzu UV-3600 with an integrating sphere. Film FTIR spectra were recorded on a Nicolet-Magna IR-850 spectrometer.

Synthesis of $[Cp_2^*Fe][PhC(O)O\text{-}B(C_6F_5)_3]$ (C1)

$[Cp_2^*Fe][PhC(O)O\text{-}B(C_6F_5)_3]$ (**C1**) was synthesized similar to reported procedure.[2] 16.5 mg of decamethylferrocene (Cp_2^*Fe) was dissolved in 1.5 mL anhydrous dichloromethane in a 20 mL amber vial in a N_2 glovebox. BCF (25.9 mg) was dissolved separately in 1.5 mL dichloromethane and added to the Cp_2*Fe reaction vial. BPO (6.23 mg) was dissolved in 0.5 mL dichloromethane, and this solution was added dropwise over 30 s to the reaction vial stirring at 400 rpm. The reaction mixture was stirred at room temperature at 600 rpm for 1 h. Then, 6 mL of anhydrous pentane was added to the reaction vial. The precipitating mixture was stirred at room temperature at 600 rpm for 25 m. The vial was removed from the glovebox to stir 350 rpm in an ice bath for 15 m. Finally, the solid was filtered from the mixture, washed with pentane, and dried by vacuum filtration in air.

NMR Spectroscopy

All spectra were recorded on a Varian VNMRS 600 MHz spectrometer at room temperature. Reaction mixture NMR solutions were prepared in a N_2 glovebox and transferred to glass screw-cap 500 Hz NMR tubes for measurement.

The initial solutions for most NMR reaction mixtures were RRa-P3HT (5 mg/mL), BCF (32.2 mg/mL), and BPO (7 mg/mL) in CD_2Cl_2. RRa-P3HT mixtures were diluted to 2.5 mg/mL. The BCF + 0.5 eq. BPO mixture was diluted to 8 mg/mL BCF and 1.75 mg/mL BPO. Reaction mixtures were stirred at room temperature at 300 rpm for 21 h before transfer to NMR tubes.

The RRa-P3HT + 0.3 eq. BCF mixture prep started with RRa-P3HT dissolved in CD_2Cl_2 at 0.5 mg/mL. Diluting CD_2Cl_2 and BCF solution in CD_2Cl_2 were added so that the reaction solution RRa-P3HT concentration was 0.33 mg/mL. The reaction mixture was stirred at room temperature at 300 rpm for 1 h before transfer to NMR tube.

^{1}H-NMR spectra in CD_2Cl_2 were calibrated to TMS, and those in $CDCl_3$ were calibrated to residual $CHCl_3$. ^{19}F-NMR spectra were calibrated to $CFCl_3$ by VnmrJ software.

Thin Film Preparation

P3HT solutions were prepared by dissolving P3HT in chloroform at 5.56 mg/mL (i.e. 5 mg per 0.9 mL) at room temperature for about 1 h. Then, acetonitrile was added to the P3HT solution in a 1:9 v/v ratio with chloroform (i.e. 5 mg P3HT per mL of 9:1 chloroform:acetonitrile).[3] P3HT vial was shaken once to mix the acetonitrile and chloroform (otherwise the acetonitrile may float on the surface of the chloroform). This mixture was allowed to equilibrate overnight (16-24 h) stirring 300 rpm at room temperature, resulting in a thick, dark purple mixture. Doped solutions at 2.5 mg/mL P3HT in 9:1 CF:ACN were prepared by sequentially adding diluting chloroform, BCF in chloroform, BPO in chloroform, and diluting acetonitrile. Doped solutions stirred 300 rpm for 1-3 h at room temperature. Doped solutions were spun cast in a N_2 glovebox at 1000 rpm for 45 s (acceleration of 1000 rpm/s), then 3000 rpm for 30 s. No thermal annealing was performed after casting the films.

Films for conductivity measurements were cast on 15 mm x 15 mm x 1 mm quartz substrates. Films for GIWAXS were cast on native oxide silicon wafer pieces cut to approx. 15 mm x 15 mm. Quartz and silicon substrates were cleaned before film deposition by sequentially sonicating in soapy water (Alconox), DI water, acetone, and 2-propanol for 15 min each. Films for UV-Vis-NIR and FTIR spectroscopy were cast on new KBr plates (2 mm thickness x 25 mm diameter, Sigma Aldrich).

GIWAXS

BCF used was purchased from Alfa Aesar (97%) and sublimated in a N_2 glovebox before use (see ^{19}F-NMR below). Films were otherwise prepared as described above on native oxide silicon substrates. GIWAXS was recorded at beamline 11-3 at the Stanford Synchrotron Radiation Lightsource (SSRL). Scattering was recorded at a 0.1° grazing angle with a sample-detector

distance of 225 mm for 540 s under He flow. Scattering patterns were calibrated and analyzed using Igor packages NIKA[4] and WAXStools.[5]

Charge Transport Measurements

Gold contacts (80 nm) were evaporated on top of the polymer films using an Angstrom Engineering thermal evaporator. The evaporation mask contact pattern contains several sets of four lines (1 mm x 0.1 mm with 0.2 mm spacing). Room-temperature conductivity was measured under N_2 atmosphere using the four-point probe method with a Keithley 6220 precision current source and Keithley 2400. Film thicknesses were measured by scratching films with a razor blade and measuring the height difference with an Asylum MFP-3D atomic force microscope in AC mode with FORTA AFM tips.

Additional UV-Vis Spectra of P3HT

To check whether benzoyl peroxide (BPO) damages RR-P3HT in the absence of BCF, we mixed P3HT and 0.5 eq. BPO in chlorobenzene solution (**Figure S1**). The spectrum was similar to the P3HT solution, suggesting that the polymer was not destroyed under these conditions. In a film cast from 9:1 CF:ACN solution, the spectrum of the P3HT + 0.5 eq. BPO mixture blueshifted and had weaker vibronic peaks, suggesting that the P3HT may be damaged or prevented from aggregation by BPO.

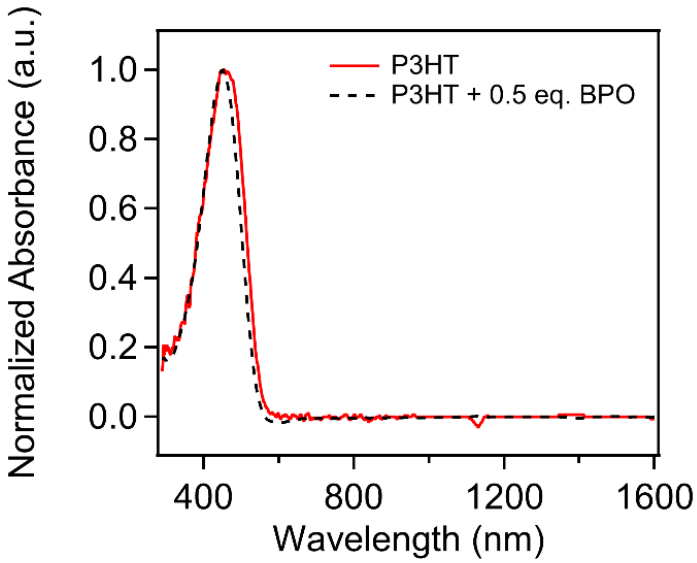

Figure S1. Normalized absorbance spectra of P3HT and P3HT + 0.5 eq. BPO in chlorobenzene solution.

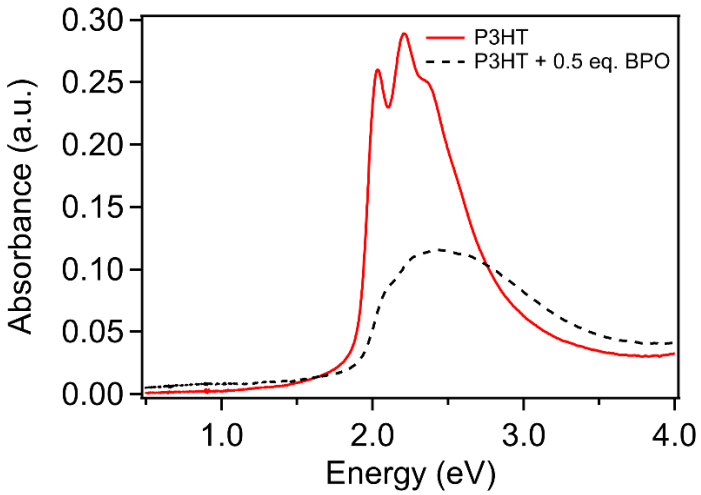

Figure S2. UV-Vis-NIR spectra of P3HT and P3HT + 0.5 eq. BPO films cast from 9:1 CF:ACN on quartz substrates.

NMR Spectroscopy

Comparison of Key Spectral Regions in ^{1}H- and ^{19}F-NMR of undoped and doped materials

Figure S3 shows the aromatic region of the ^{1}H-NMR spectra (left) and the ^{19}F-NMR spectra (right) of solutions of precursors, controls, and doped solutions of RRa-P3HT with BCF and BPO. The full spectra presented in **Figures S4-S18** along with the spectra of precursors used in the experiments.

The ^{1}H-NMR spectrum of $[Cp_2^*Fe]^+$:$[PhC(O)O\text{-}B(C_6F_5)_3]^-$ (**C1**) has peaks at 8.11 (d), 7.55 (d), and 7.50 ppm (d), matching the previous synthesis (**Figure S3** and **S7**).[2] **C1** has three signals in its ^{19}F-NMR spectrum at -135, -163.4, and -167.6 ppm, consistent with the reported synthesis (**Figure S3** and **S8**).[2] The smaller second set of peaks in the spectrum for **C1**, at -136, -160, and -166 ppm, are likely from wet BCF. If excess unreacted BCF remained in the sample of **C1**, that excess BCF would have absorbed water when the **C1** solid was washed and filtered in air.

The ^{1}H-NMR spectrum of the RRa-P3HT + 0.1 eq. BCF:BPO solution is difficult to assign due to the number of peaks and we note that some products from BCF and CD_2Cl_2 will not be present due to the lack of ^{1}H nuclei. (**Figure S3**, **Figure S10,** and **Figure S11**). Here we assign the spectra as best as possible although there are significant uncertainties with some assignments. One doublet and two triplets in this spectrum (red dashed lines) have coupling similar to that of **C1** but are shifted upfield by 0.1-0.15 ppm (red arrows). These peaks are tentatively assigned to the predicted counterion, given that changes in electronic distribution may have shifted the peaks. A second set of one doublet and two triplets in the RRa-P3HT + 0.1 eq. BCF:BPO spectrum most closely matches the positions of broad peaks in the RRa-P3HT + 0.05 eq. BPO spectrum, suggesting there are side reactions between RRa-P3HT and BPO. Small peaks in the RRa-P3HT + 0.1 eq. BCF:BPO spectrum at 8.34 and 8.26 ppm match doublet locations in the BCF + 0.5 eq. BPO spectrum, suggesting that some BCF-BPO complexes are also present.

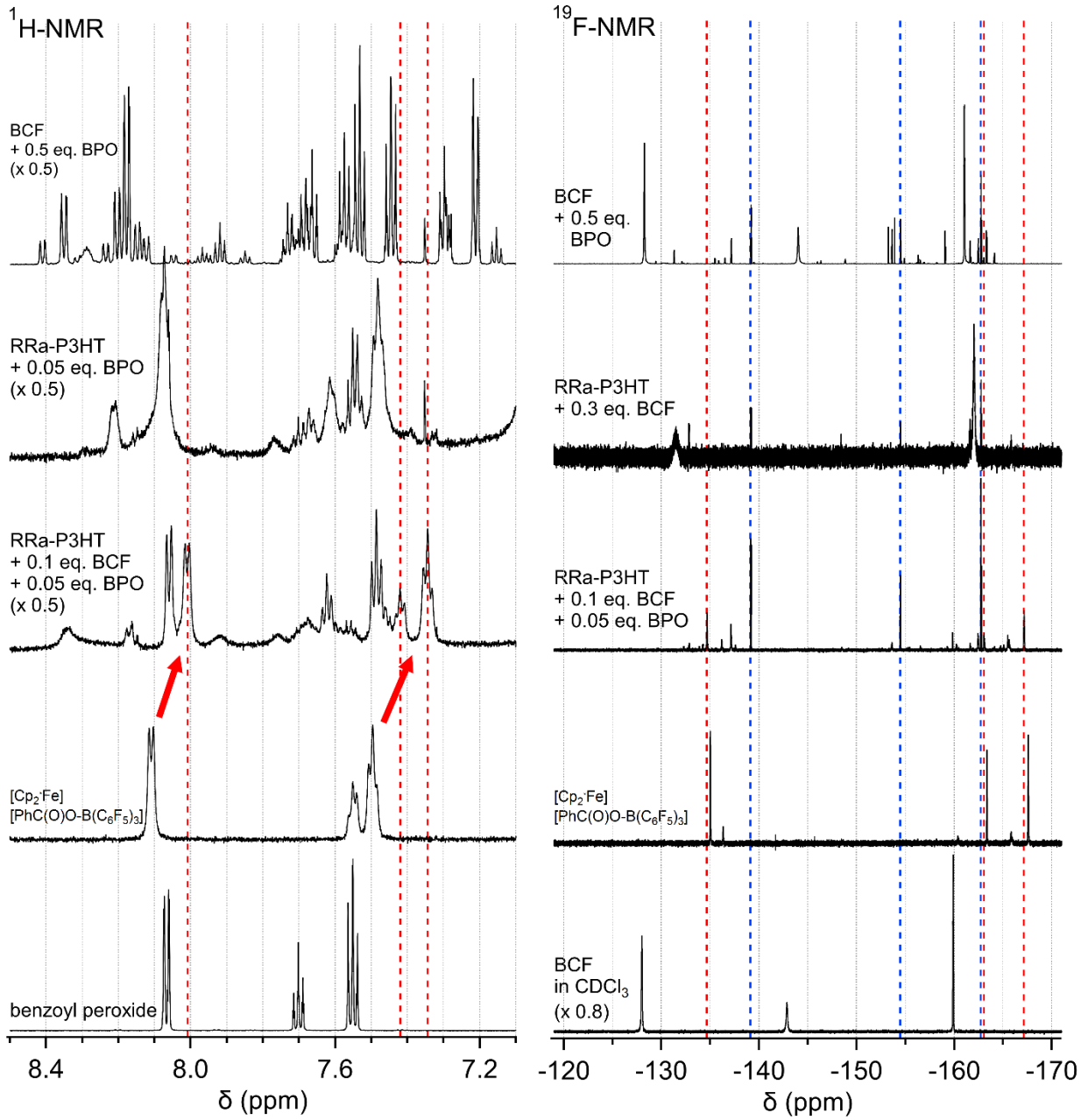

Figure S3. ^{1}H- and ^{19}F-NMR spectra of BCF- and BPO-doped RRa-P3HT and relevant control solutions in CD_2Cl_2 (except BCF solution in $CDCl_3$). Red dashed lines indicate peaks attributed to [PhC(O)O-$B(C_6F_5)_3$] doping product. Blue dashed lines indicate common side reaction product.

$B(C_6F_5)_3$

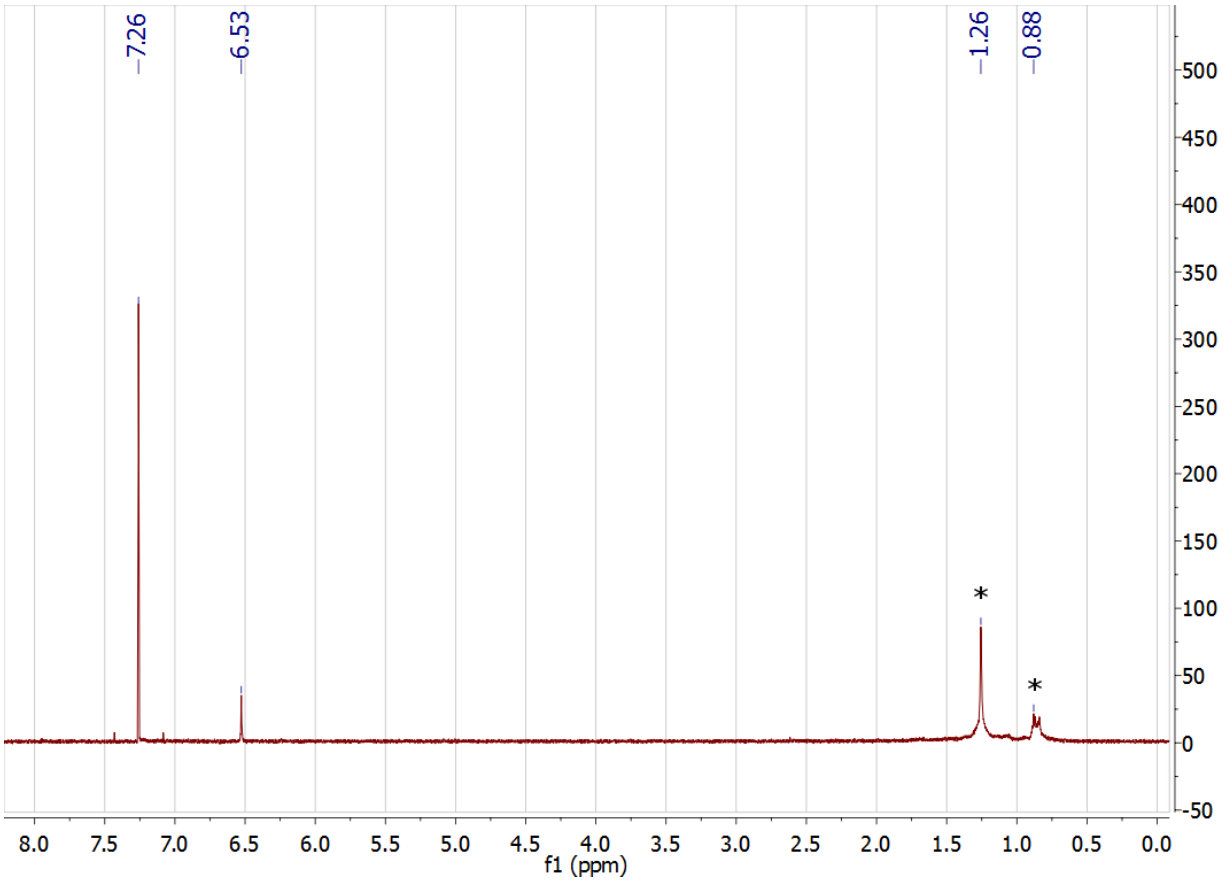

Figure S4. ^{1}H-NMR spectrum of BCF (TCI America, after opening) in $CDCl_3$. Asterisks indicate hydrocarbon grease introduced during sample prep.

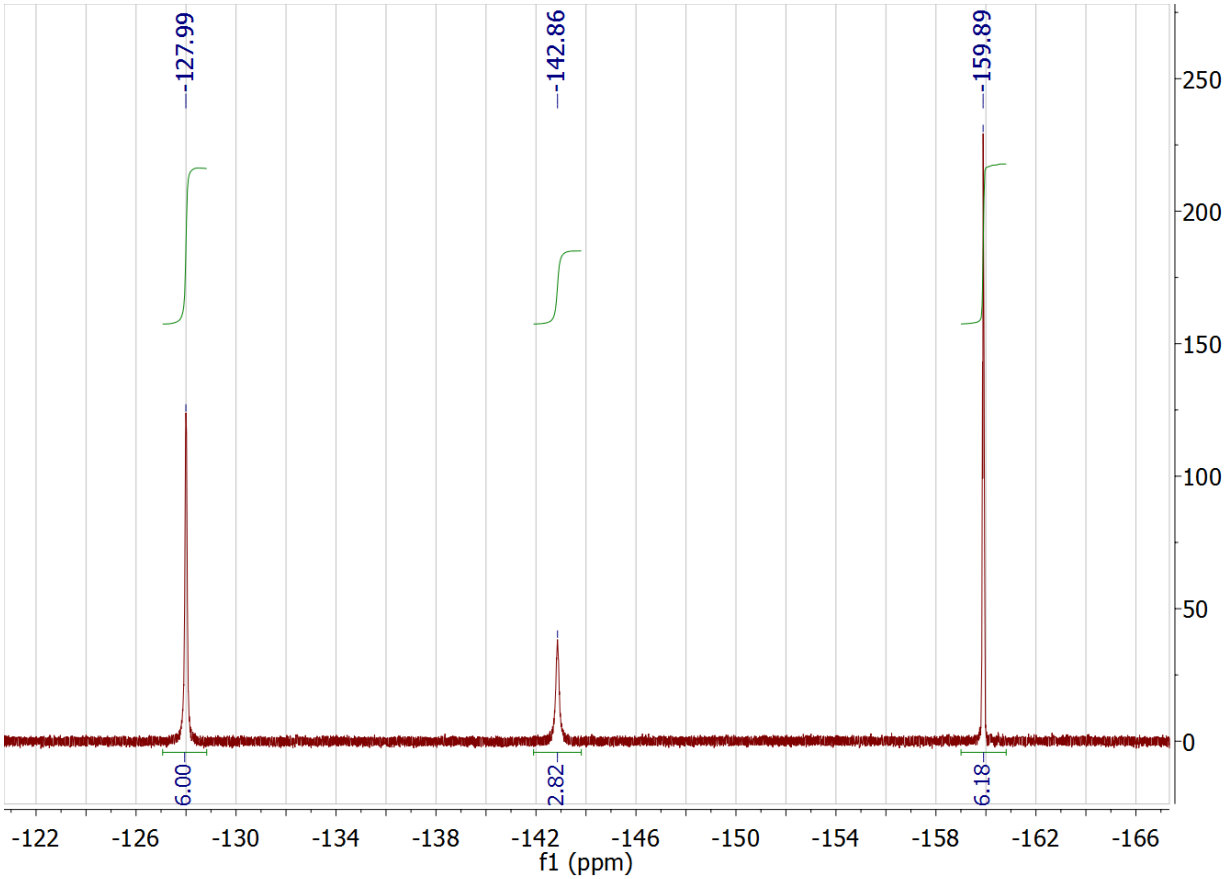

Figure S5. ^{19}F-NMR spectrum of BCF (TCI America, after opening) in $CDCl_3$.

Benzoyl Peroxide

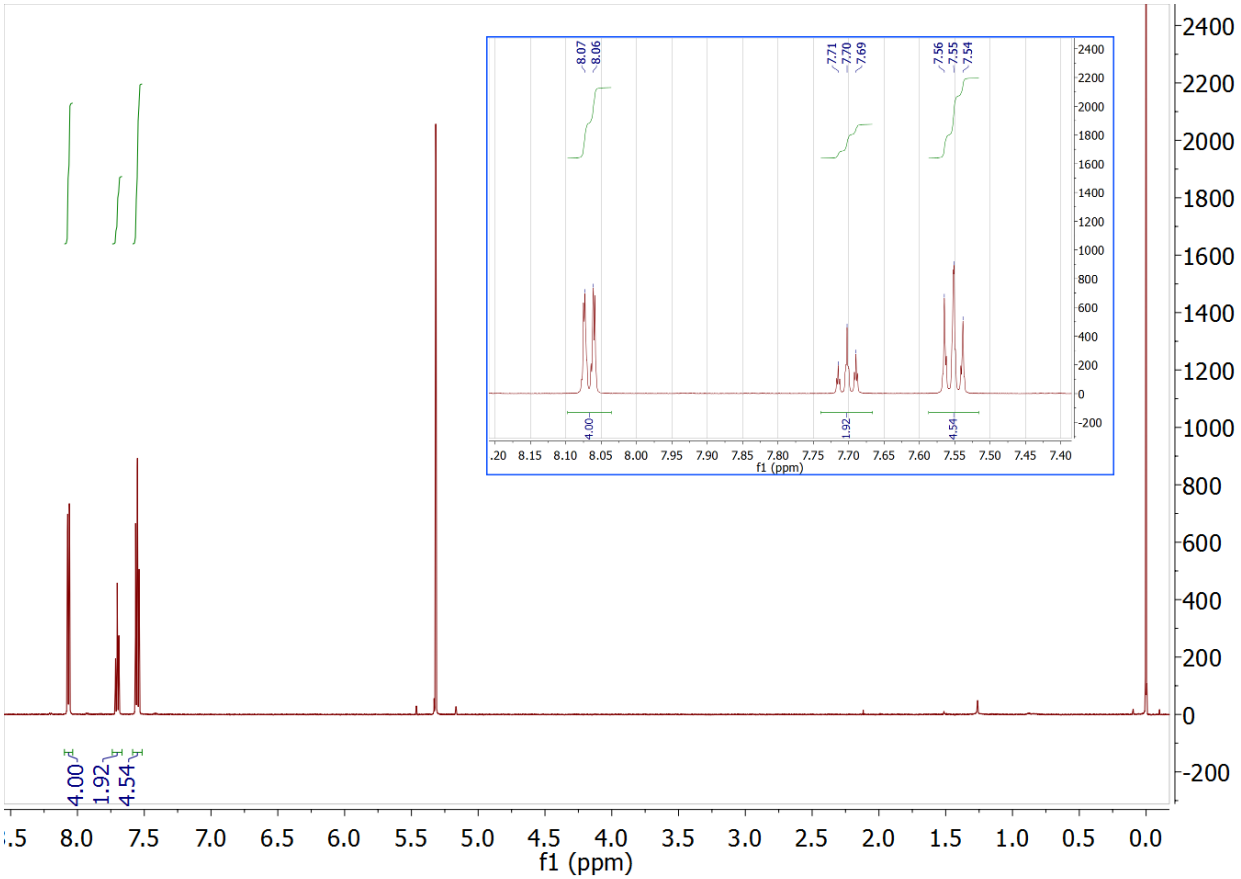

Figure S6. ^{1}H-NMR spectrum of benzoyl peroxide in CD_2Cl_2. Inset highlights aromatic peaks.

[Cp_2^*Fe][PhC(O)O-B(C_6F_5)$_3$] (C1)

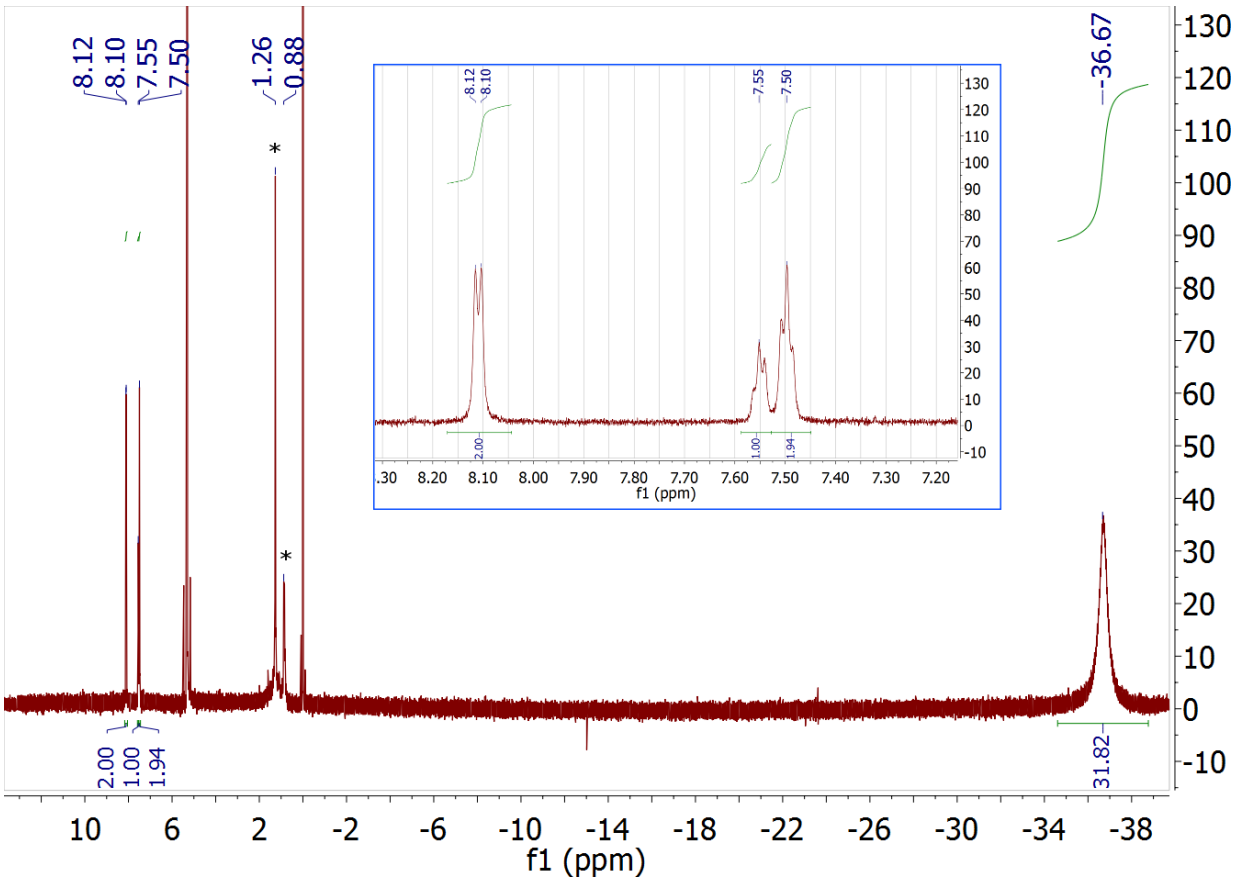

Figure S7. ^{1}H-NMR spectrum of **C1** in CD_2Cl_2. Asterisks indicate hydrocarbon grease. Inset highlights aromatic peaks.

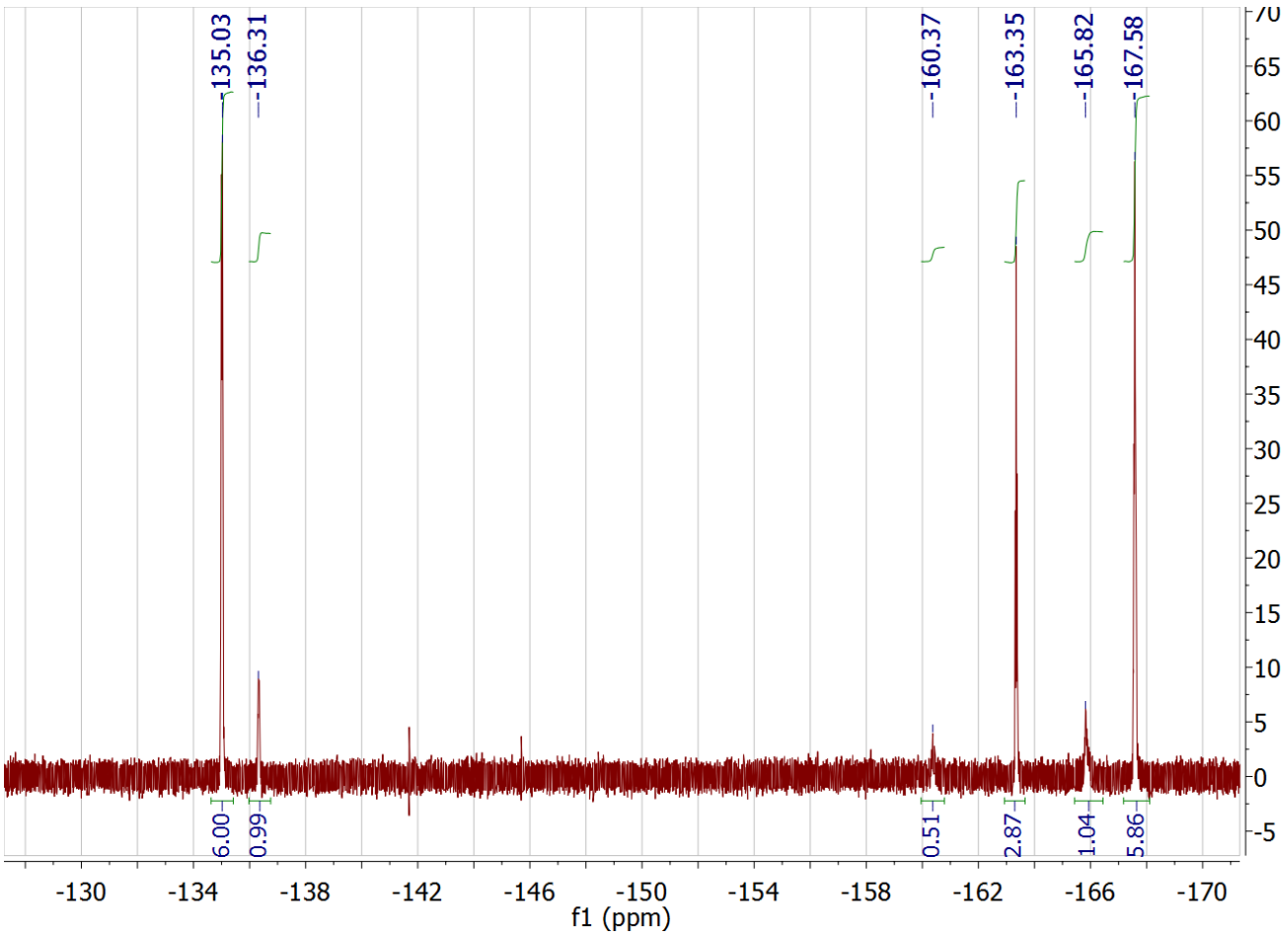

Figure S8. ^{19}F-NMR spectrum of **C1** in CD_2Cl_2.

RRa-P3HT

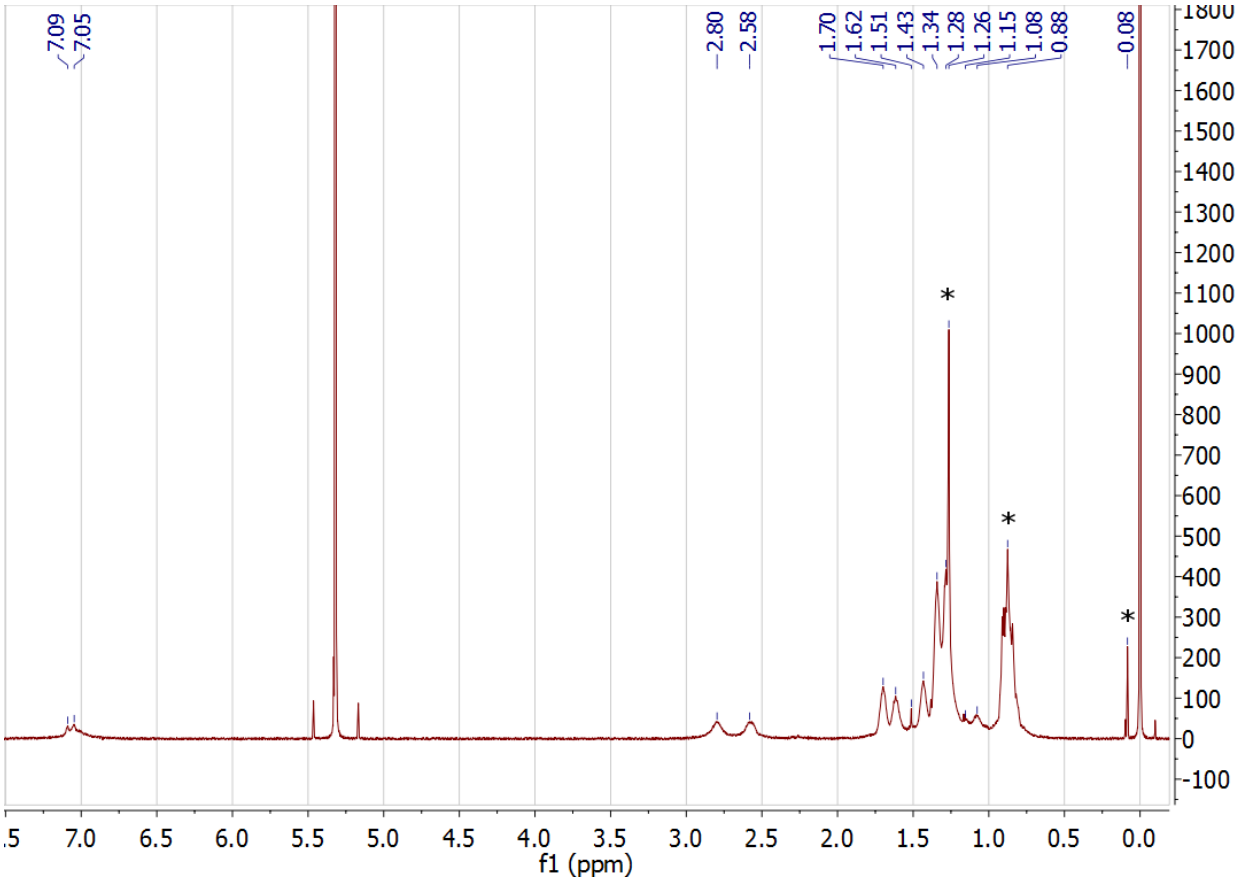

Figure S9. ^{1}H-NMR spectrum of RRa-P3HT in CD_2Cl_2. Asterisks indicate hydrocarbon grease and silicone grease.

RRa-P3HT + 0.1 eq. BCF:BPO

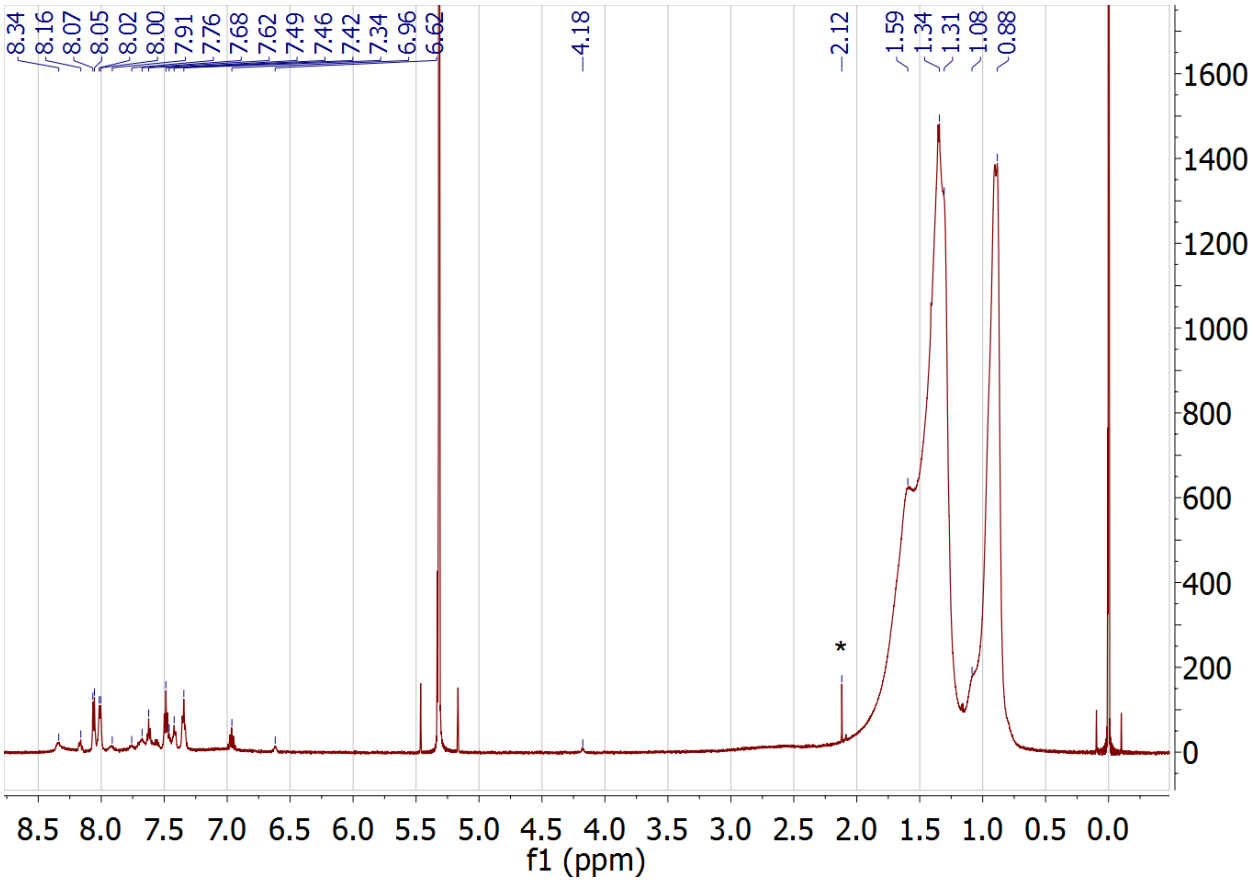

Figure S10. ^{1}H-NMR spectrum of RRa-P3HT + 0.1 eq. BCF:BPO in CD_2Cl_2. Asterisk indicates acetone.

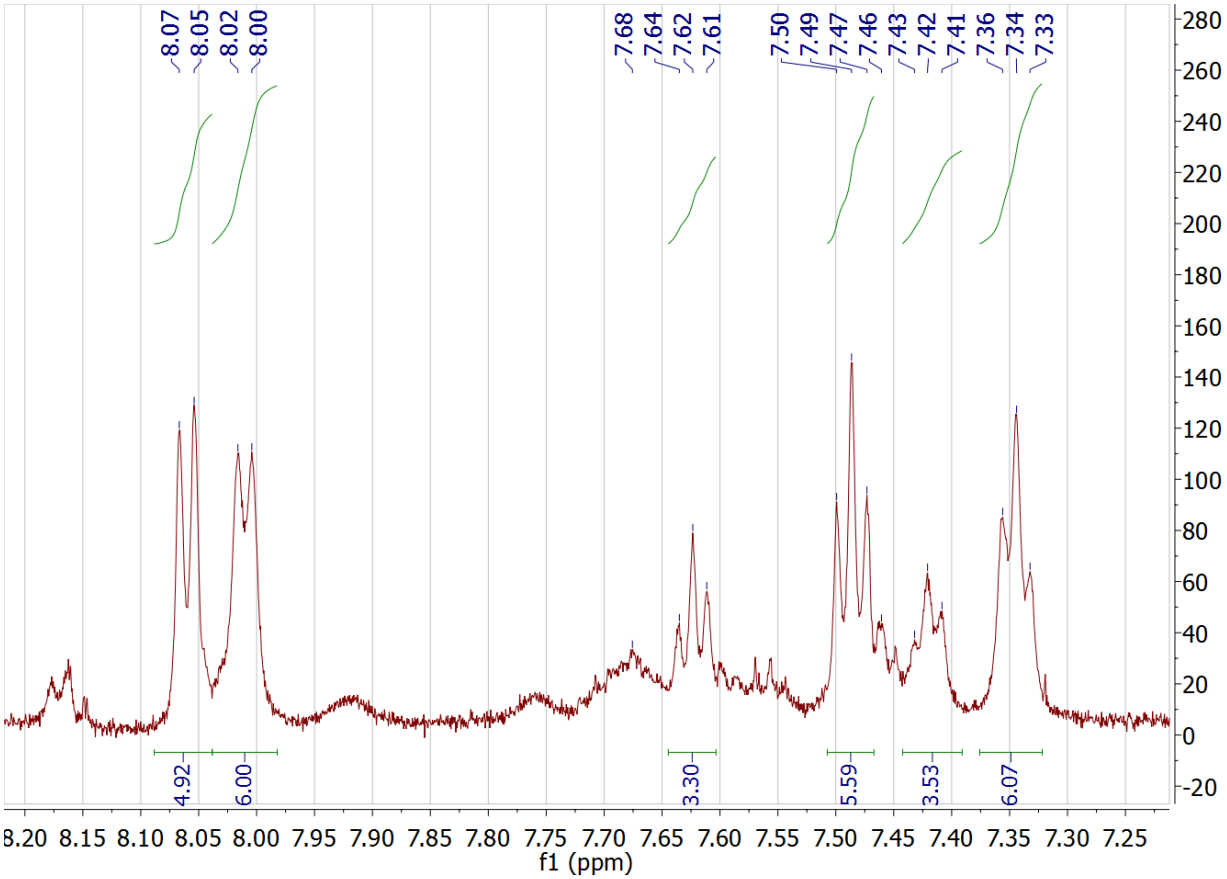

Figure S11. Aromatic region of ^{1}H-NMR spectrum of RRa-P3HT + 0.1 eq. BCF:BPO in CD_2Cl_2.

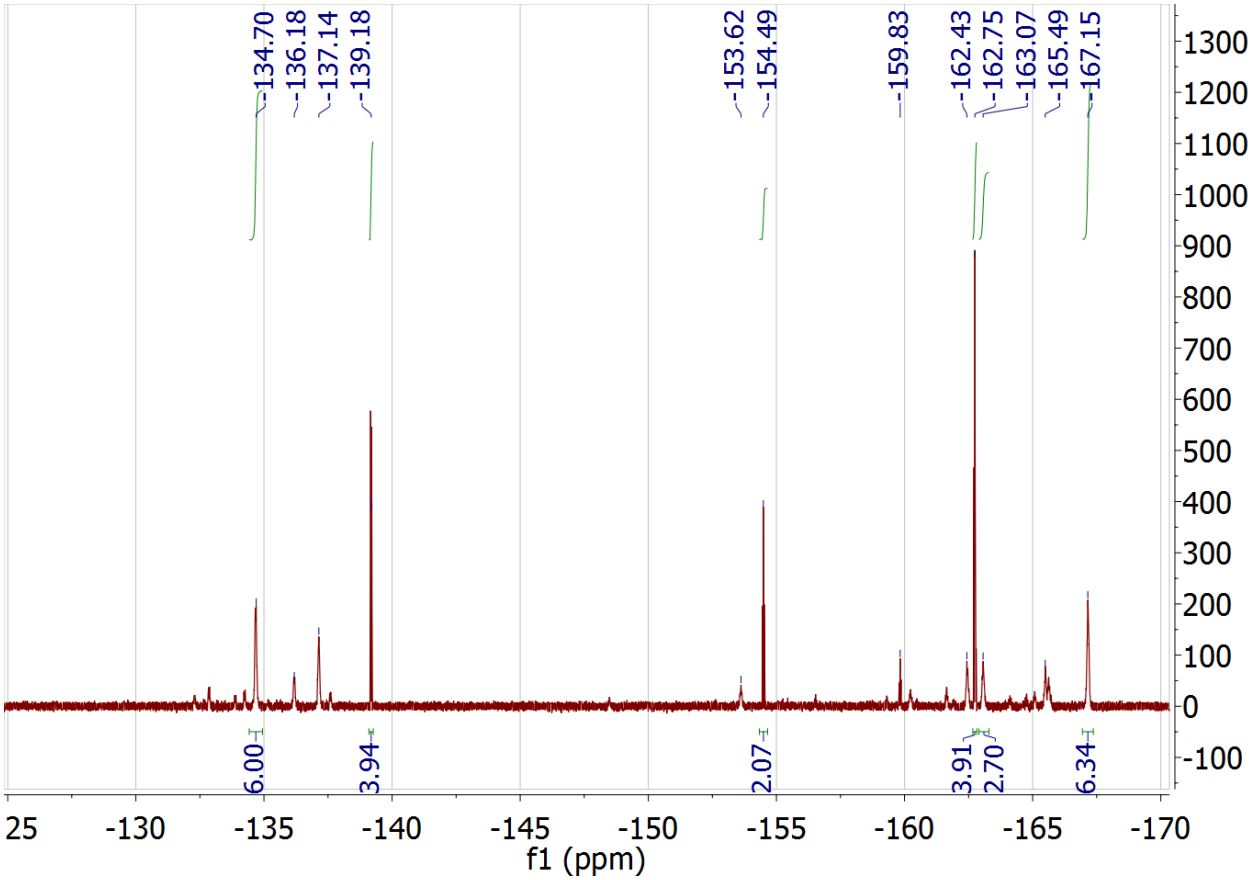

Figure S12. ^{19}F-NMR spectrum of RRa-P3HT + 0.1 eq. BCF:BPO in CD_2Cl_2.

RRa-P3HT + 0.3 eq. BCF

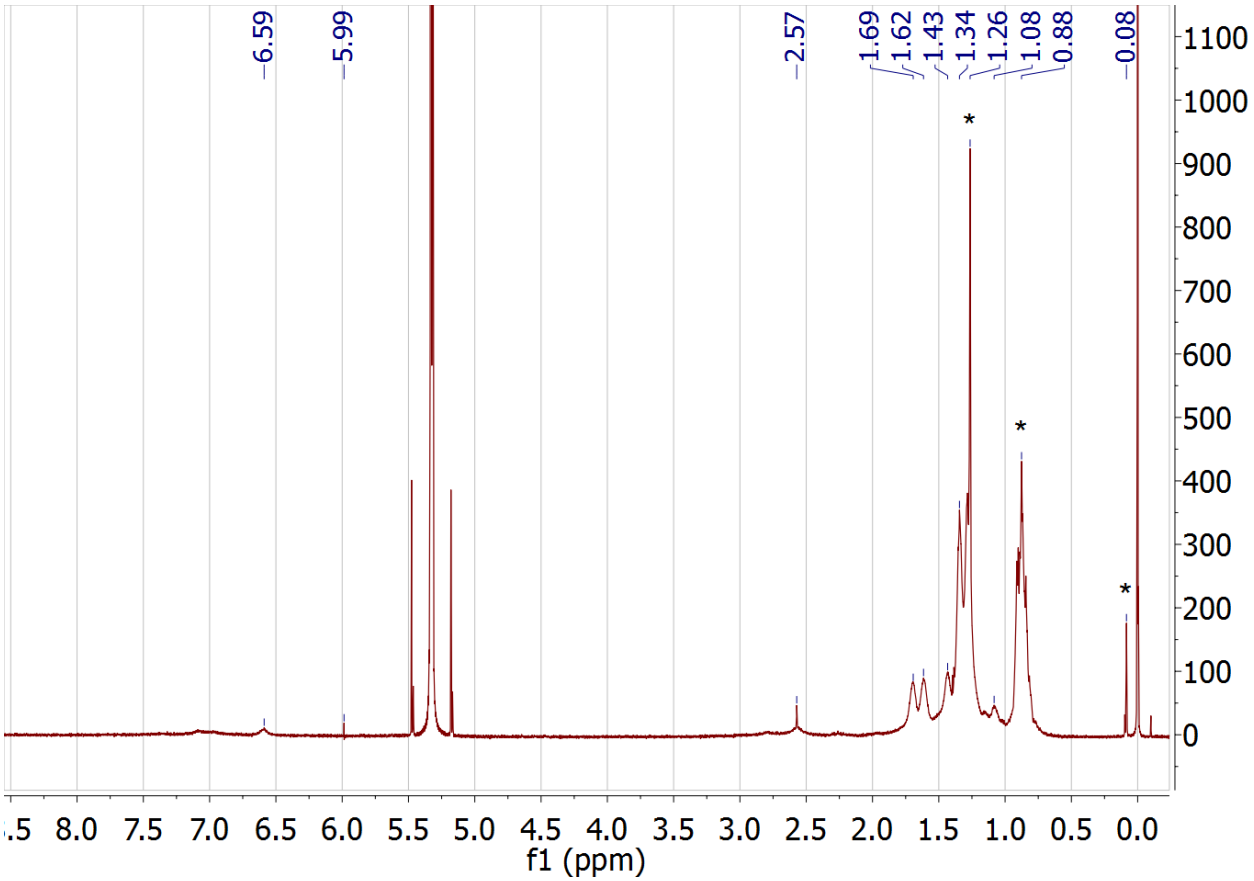

Figure S13. ^{1}H-NMR spectrum of RRa-P3HT + 0.3 eq. BCF in CD_2Cl_2. Asterisks indicate hydrocarbon grease and silicone grease.

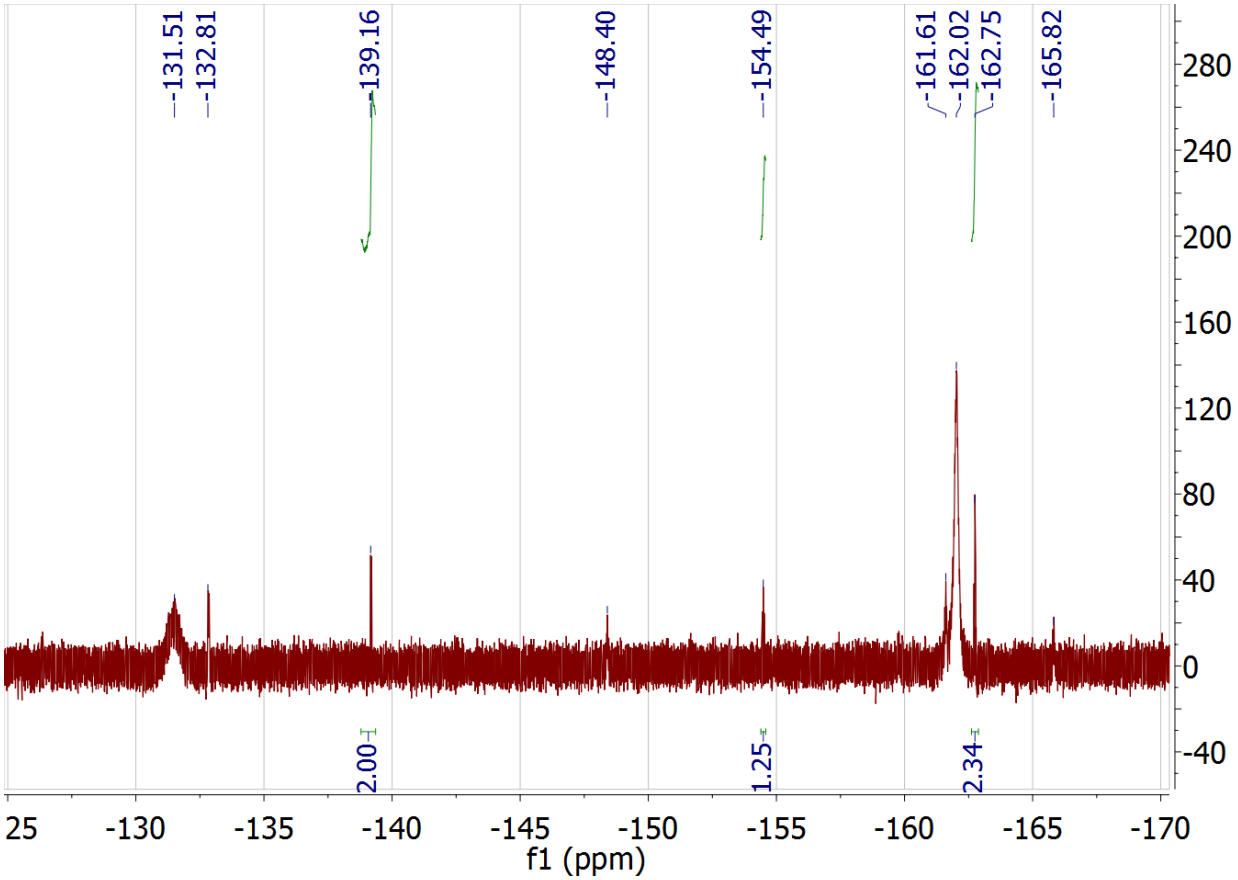

Figure S14. ^{19}F-NMR spectrum of RRa-P3HT + 0.3 eq. BCF in CD_2Cl_2.

RRa-P3HT + 0.05 eq. BPO

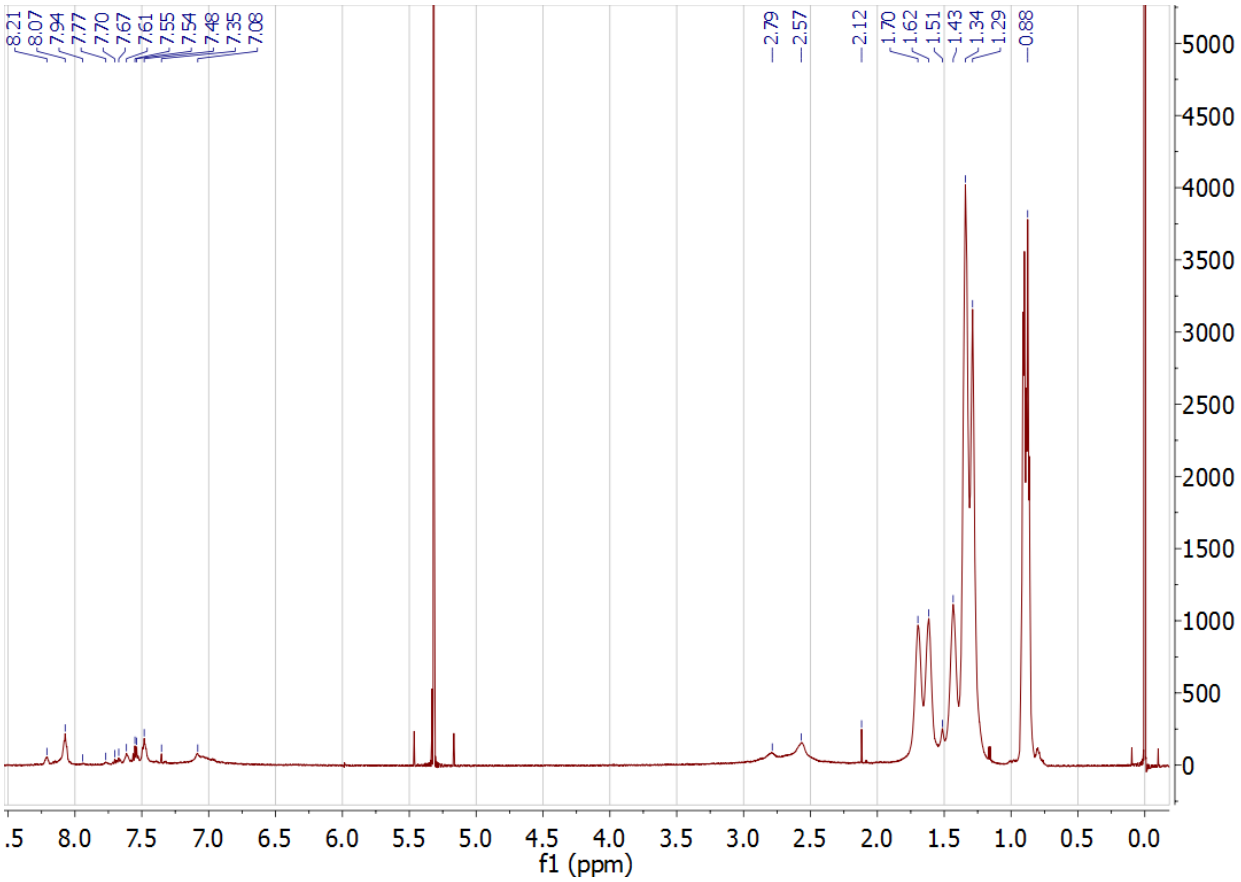

Figure S15. RRa-P3HT + 0.05 eq. BPO in CD_2Cl_2.

BCF + 0.5 eq. BPO

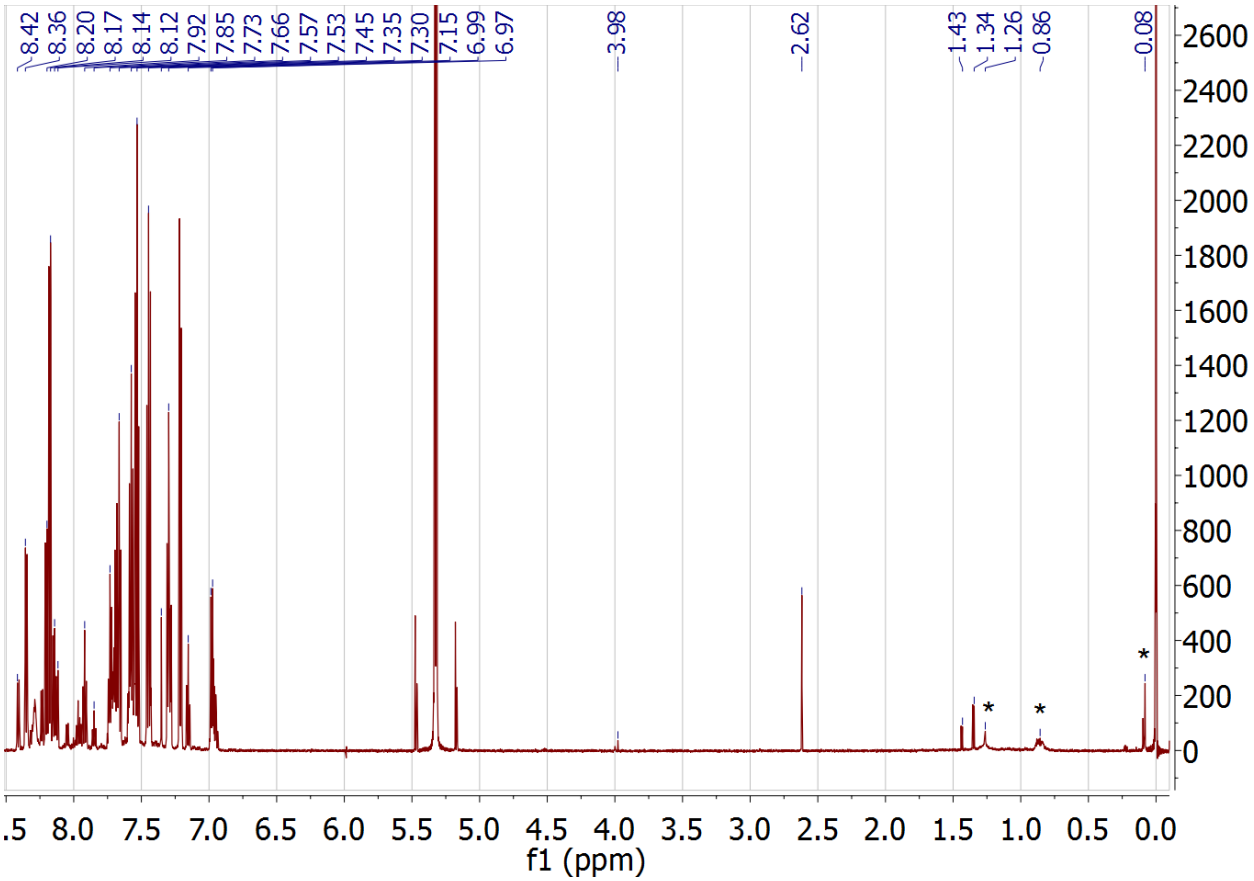

Figure S16. ^{1}H-NMR spectrum of BCF + 0.5 eq. BPO in CD_2Cl_2. Asterisks indicate hydrocarbon grease and silicone grease.

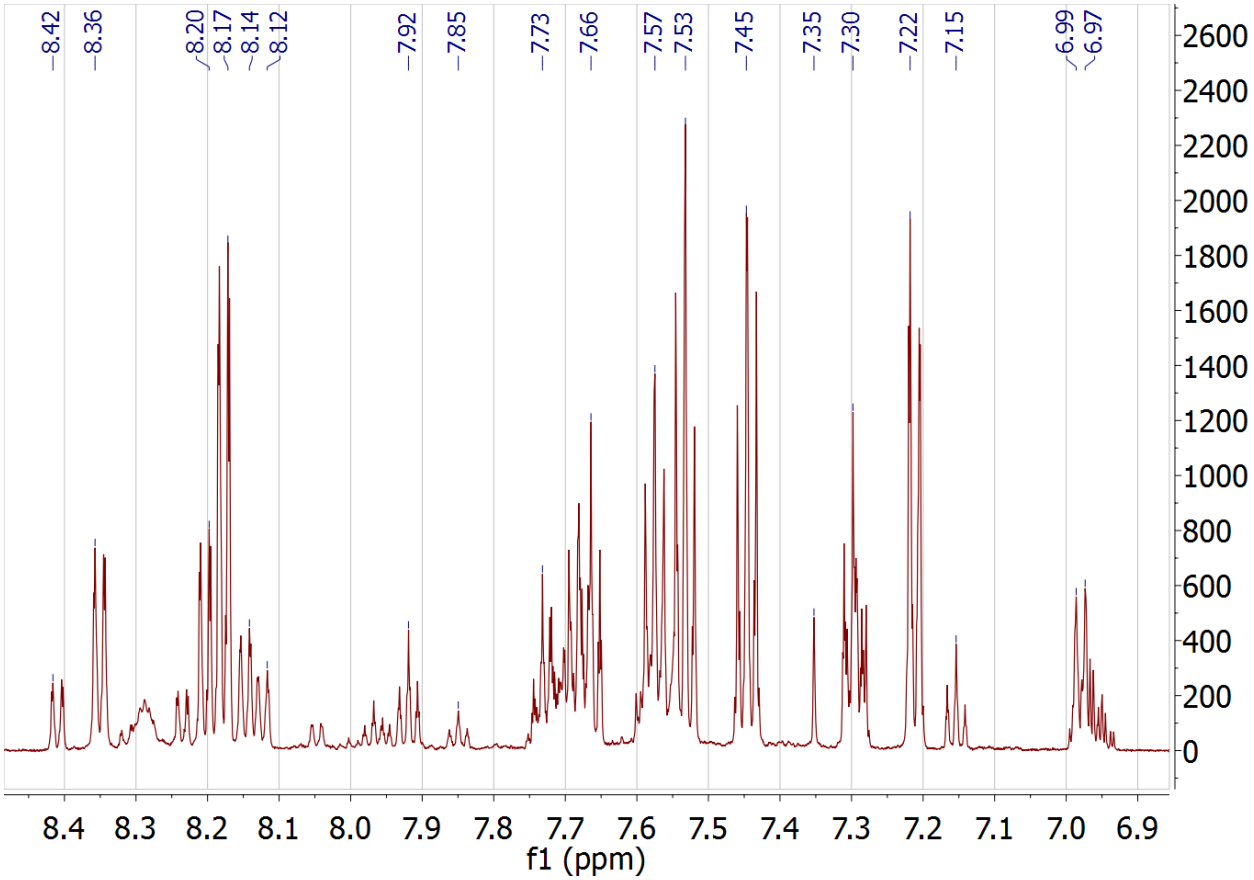

Figure S17. Aromatic region of ^{1}H-NMR spectrum of BCF + 0.5 eq. BPO in CD_2Cl_2.

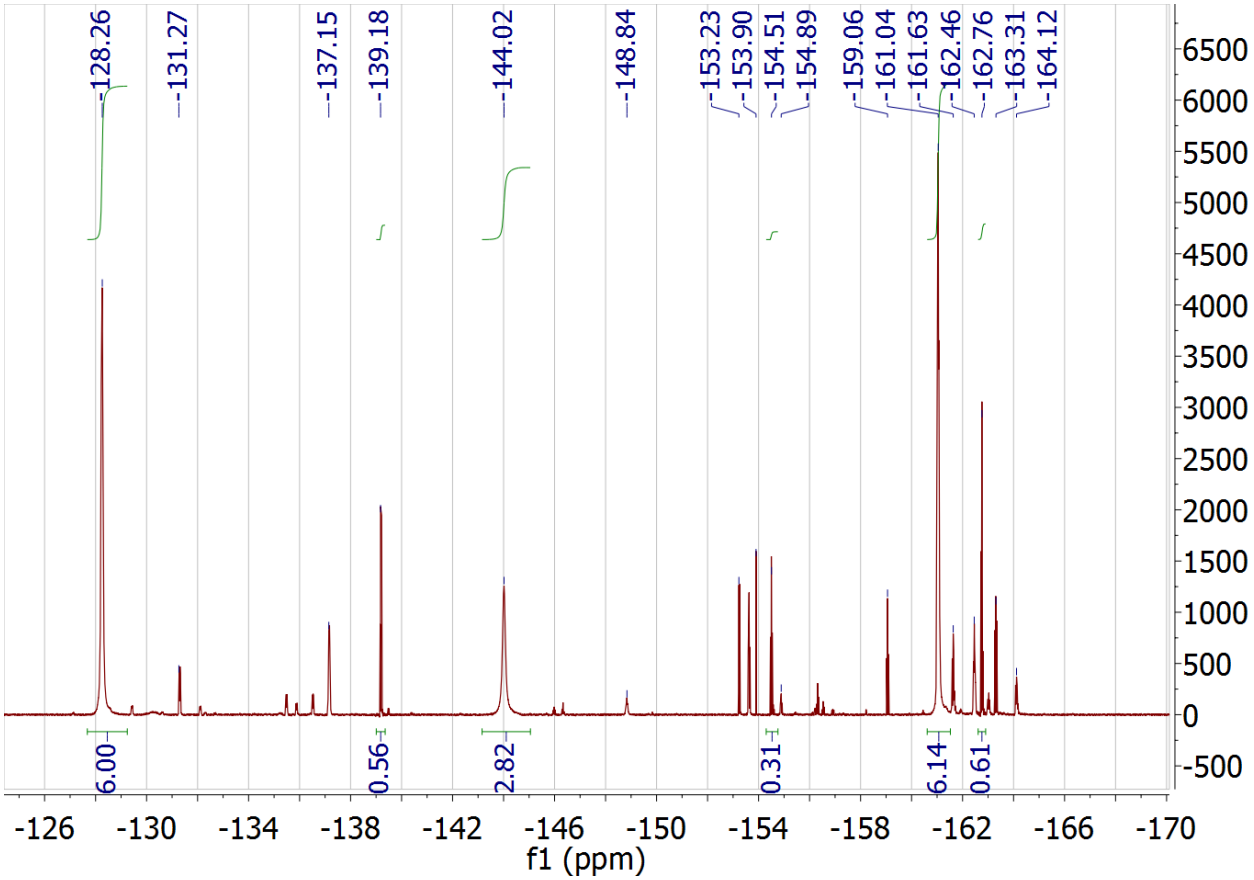

Figure S18. ^{19}F-NMR spectrum of BCF + 0.5 eq. BPO in CD_2Cl_2.

NMR Spectra of BCF and UV-Vis Spectra of Doped Conjugated Polymers

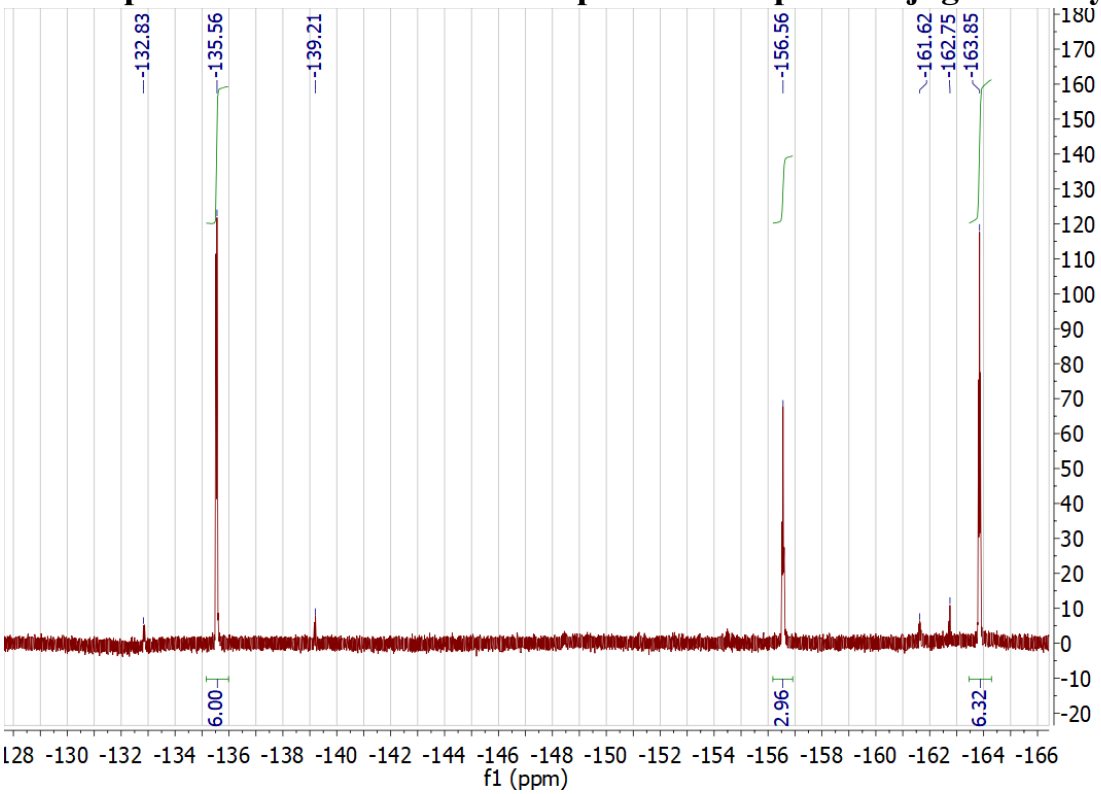

Figure S19. ^{19}F-NMR spectrum of air-exposed BCF (95%, Sigma Aldrich) used to dope MEH-PPV, IDTBT, and PFO.

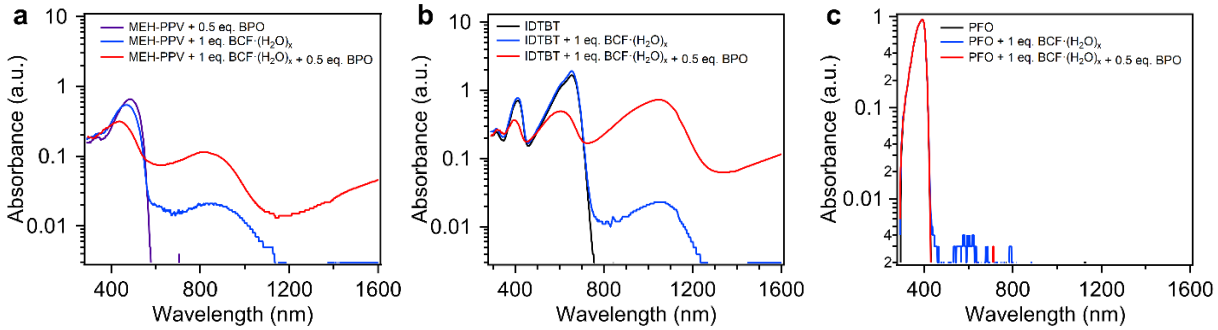

Figure S20. Log scale UV-Vis spectra of doped MEH-PPV, IDTBT, and PFO solutions in chlorobenzene. (i.e. Log version of Figure 3)

Grazing Incidence Wide Angle X-ray Scattering (GIWAXS) Data

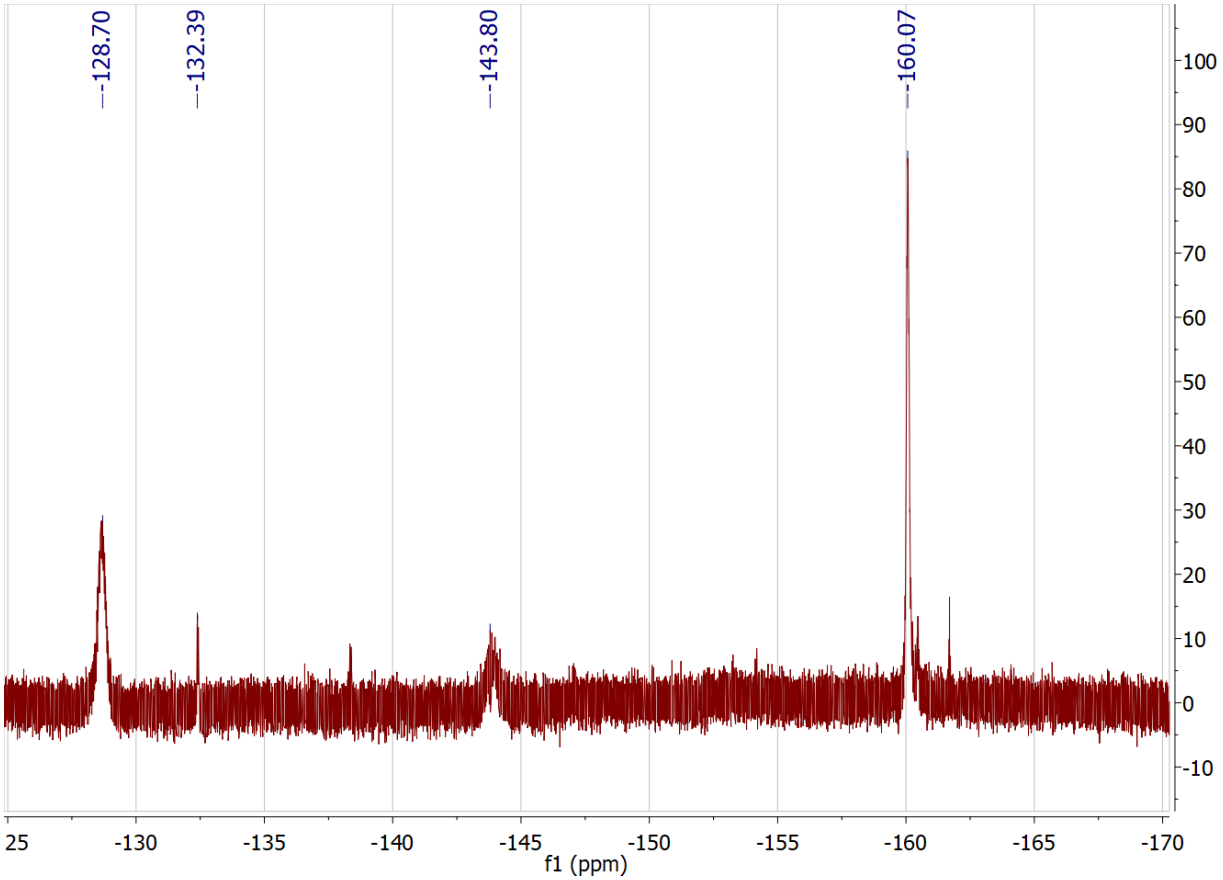

Figure S21. ^{19}F-NMR spectrum of sublimated BCF (Alfa Aesar) used for GIWAXS samples.

BCF Doping GIWAXS:	P3HT	P3HT + 0.05 eq. BCF
	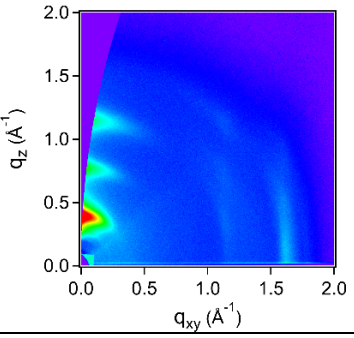	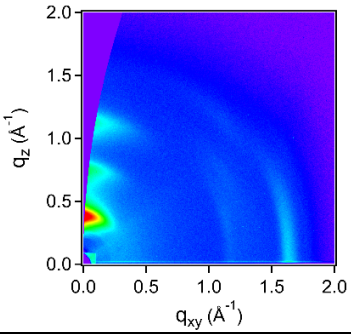
Alkyl spacing (Å)	16.2	16.7
π-π spacing (Å)	3.88	3.85
P3HT + 0.1 eq. BCF	P3HT + 0.2 eq. BCF	P3HT + 0.3 eq. BCF
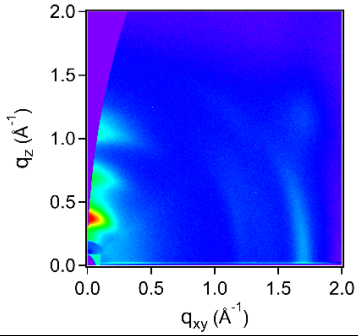	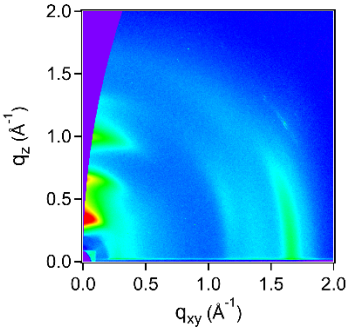	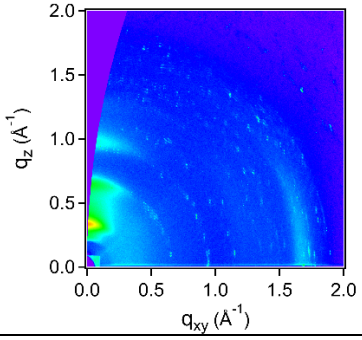
17.0	18.3	18.8
3.70	3.78	3.75

Figure S22. GIWAXS images of BCF-doped RR-P3HT films.

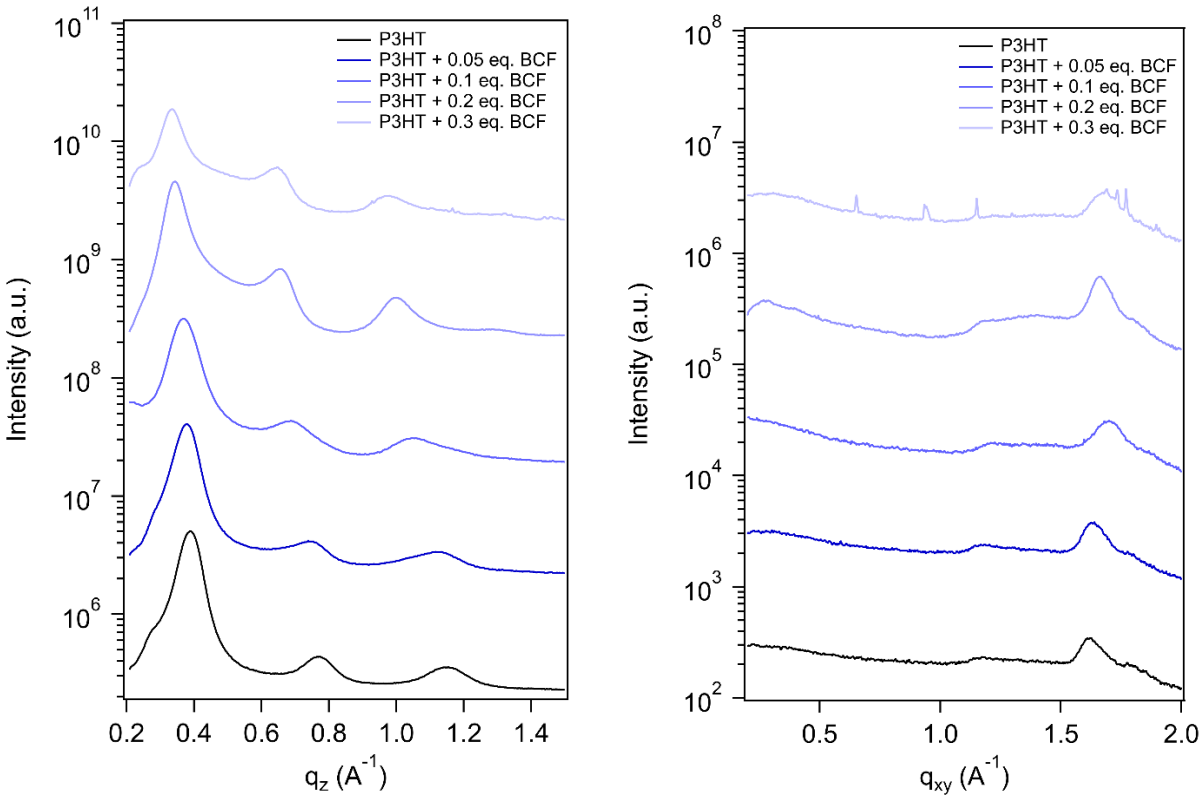

Figure S23. GIWAXS linecuts of BCF-doped RR-P3HT (left) out-of-plane and (right) in-plane.

BCF:BPO Doping	P3HT	P3HT + 0.05 eq. BCF:BPO
	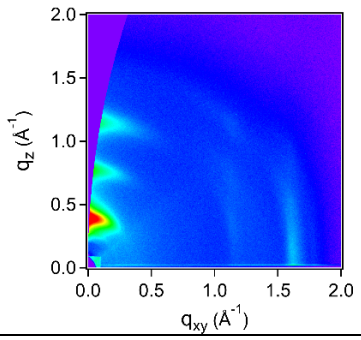	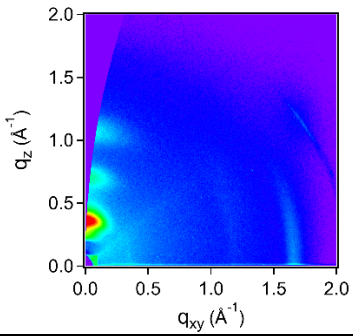
Alkyl spacing (Å)	16.2	17.5
π-π spacing (Å)	3.88	3.79
P3HT + 0.1 eq. BCF:BPO	P3HT + 0.2 eq. BCF:BPO	P3HT + 0.3 eq. BCF:BPO
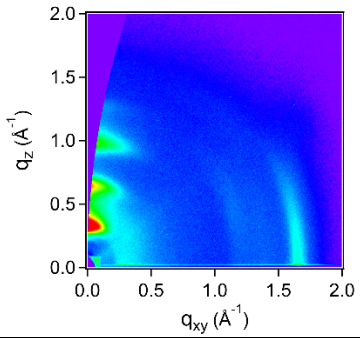	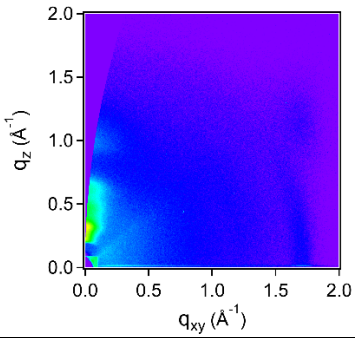	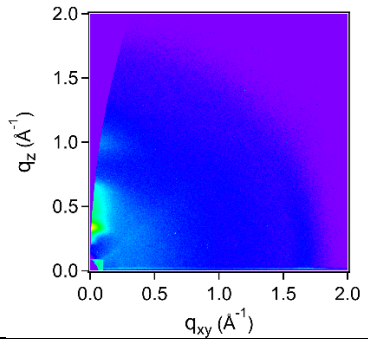
19.0	19.5	18.5
3.80	3.67	3.75

Figure S24. GIWAXS images of BCF:BPO-doped RR-P3HT films. BCF:BPO-doped images are on a narrower color scale than the neat film and BCF-doped images.

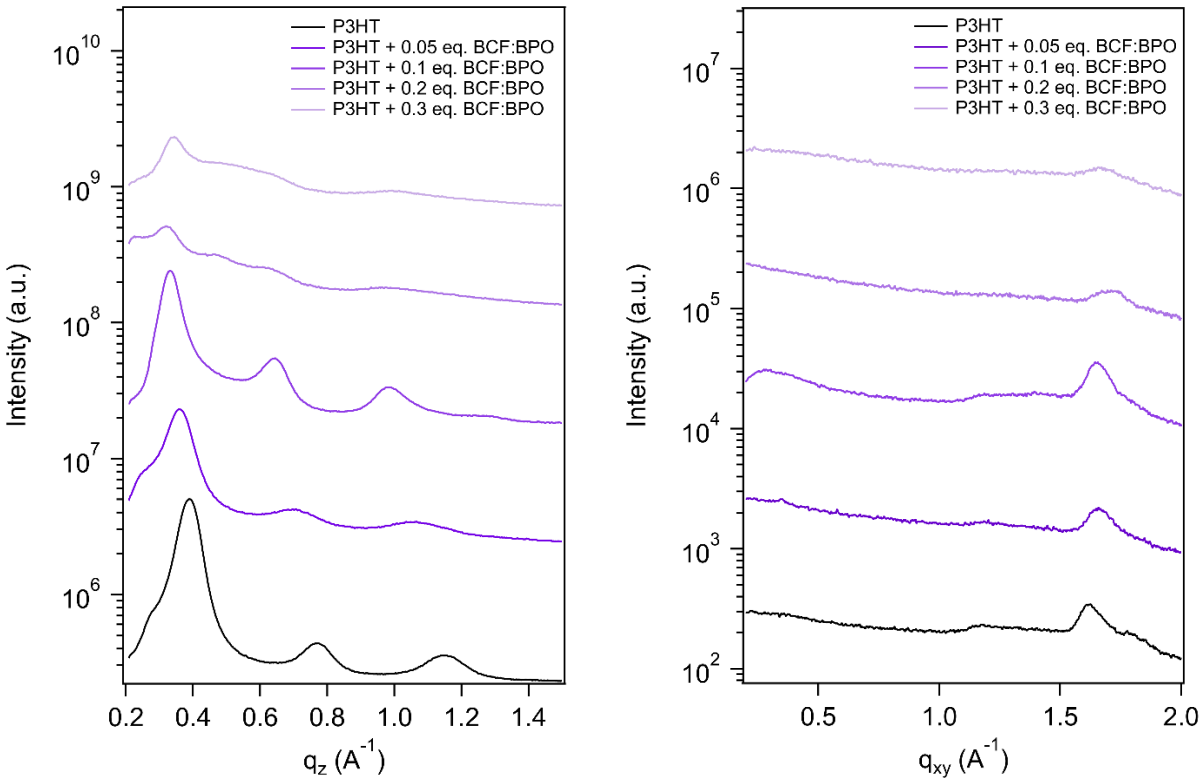

Figure S25. GIWAXS linecuts of BCF:BPO-doped RR-P3HT (left) out-of-plane and (right) in-plane.

Near-infrared and Infrared Spectra of Doped Films

To better understand the change in shape of the polaron peak (0.05-1.0 eV) with doping, we used several Gaussian peaks to fit this peak. The FTIR and NIR spectra between 0.055 – 1.0 eV of each film were fitted with 15 gaussian peaks using the IgorPro Multipeak Fitting 2 package. A constant baseline was manually set near the absorbance value at 1.0 eV. After using the "Auto-locate peaks" function to generate initial guesses for the IRAV (#4-11) and C-H stretch (#12-14) fitting functions, guesses for the broader functions (#0-3) were manually entered (**Figure S26**). During the fitting, peak locations, heights, and widths were allowed to vary freely (**Tables S1, S2**). Peak #3 (B3), representing the blue side of P2b, increased disproportionately to the other peaks (**Figure S27**), suggesting that the proportion of localized polarons increases with doping. However, this empirical area calculation may not reflect the actual electronic transitions or the polaron model.[6]

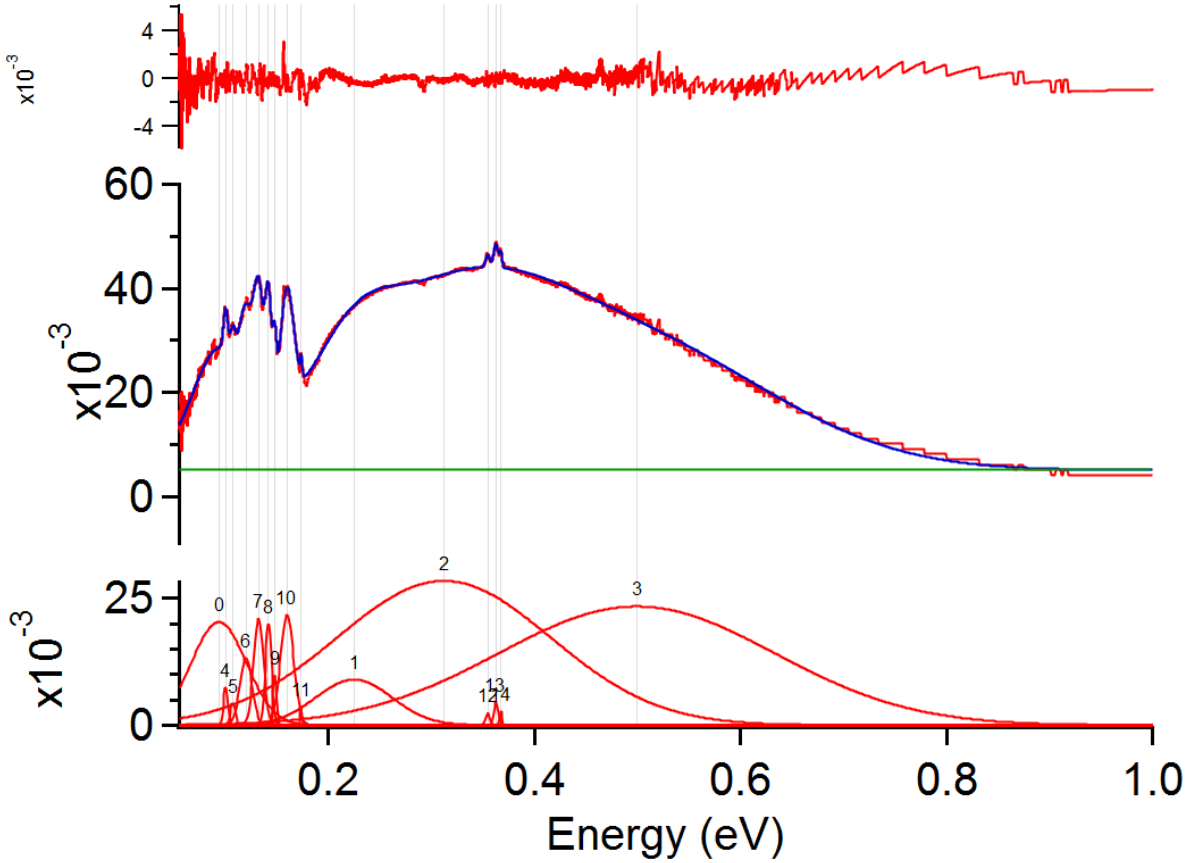

Figure S26. Example of Gaussian fitting of FTIR and NIR spectra of P3HT + 0.05 eq. BCF:BPO film.

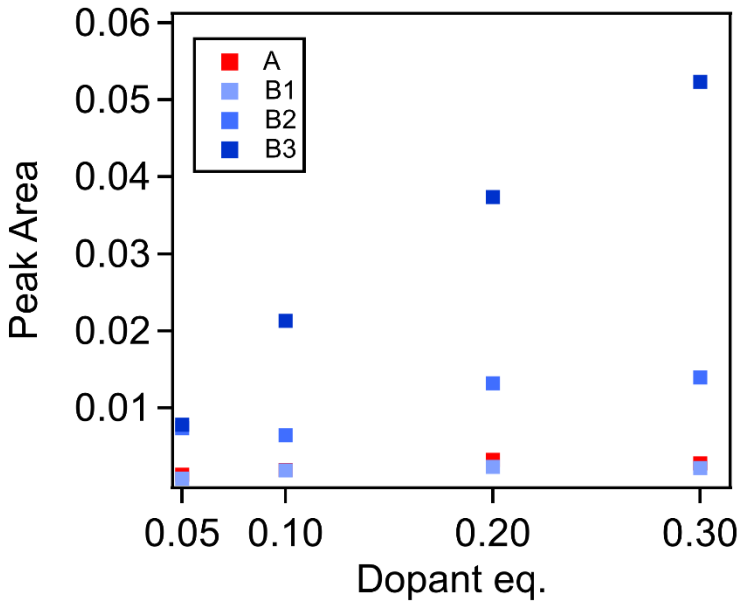

Figure S27. Comparison of how the areas of the four polaron peak fitting functions change with doping.

Table S1. Comparison table of polaron fitting peak location changes with doping.

Peak Locations	A (eV)	B1 (eV)	B2 (eV)	B3 (eV)
+ 0.05 eq. BCF:BPO	0.093293	0.224423	0.311881	0.499107
+ 0.1 eq. BCF:BPO	0.093223	0.222113	0.309044	0.436165
+ 0.2 eq. BCF:BPO	0.089265	0.217534	0.293467	0.466241
+ 0.3 eq. BCF:BPO	0.089129	0.220794	0.289218	0.467767

Table S2. Comparison table of polaron fitting peak area changes with doping, used to plot Figure S25.

Peak Areas	A	B1	B2	B3
+ 0.05 eq. BCF:BPO	0.001358	0.000835	0.007396	0.007843
+ 0.1 eq. BCF:BPO	0.00195	0.001878	0.006477	0.021319
+ 0.2 eq. BCF:BPO	0.003292	0.002378	0.013209	0.037385
+ 0.3 eq. BCF:BPO	0.002832	0.002209	0.01397	0.052343

Electrical Conductivity

Table S3. Electrical conductivity of BCF- and BCF:BPO-doped RR-P3HT films, used for Figure 6.

	Conductivity (S/cm)		Conductivity (S/cm)
RR-P3HT	0.0013 ± 0.0002		
+ 0.05 eq. BCF	0.35 ± 0.07	+ 0.05 eq. BCF:BPO	0.4 ± 0.1
+ 0.1 eq. BCF	1.2 ± 0.2	+ 0.1 eq. BCF:BPO	7 ± 3
+ 0.2 eq. BCF	3.5 ± 0.5	+ 0.2 eq. BCF:BPO	25 ± 6
+ 0.3 eq. BCF	5.2 ± 0.6	+ 0.3 eq. BCF:BPO	20 ± 6

Table S4. Previously reported electrical conductivities of BCF-doped P3HT and PCPDTBT films.

Polymer	BCF doping	Conditions	Conductivity (S/cm)	Ref.
P3HT	120%	In air	33.0	[7]
P3HT	25%	In N_2	0.020	[7]
P3HT	0.25/monomer		$\sim 10^{-3}$	[8]
PCPDTBT	0.2 eq.	In N_2	8×10^{-3}	[9]
PCPDTBT	23 mol%		0.65	[10]

References

1 H. Bronstein, D. S. Leem, R. Hamilton, P. Woebkenberg, S. King, W. Zhang, R. S. Ashraf, M. Heeney, T. D. Anthopoulos, J. de Mello and I. McCulloch, *Macromolecules*, 2011, **44**, 6649–6652.

2 L. L. Liu, L. L. Cao, Y. Shao and D. W. Stephan, *J. Am. Chem. Soc.*, 2017, **139**, 10062–10071.

3 K. D. Kim, S. Park, S. Nho, G. Baek and S. Cho, *Current Applied Physics*, 2014, **14**, 1369–1373.

4 J. Ilavsky, *J. Appl. Cryst.*, 2012, **45**, 324–328.

5 S. D. Oosterhout, V. Savikhin, J. Zhang, Y. Zhang, M. A. Burgers, S. R. Marder, G. C. Bazan and M. F. Toney, *Chem. Mater.*, 2017, **29**, 3062–3069.

6 R. Ghosh, A. R. Chew, J. Onorato, V. Pakhnyuk, C. K. Luscombe, A. Salleo and F. C. Spano, *J. Phys. Chem. C*, 2018, **122**, 18048–18060.

7 E. H. Suh, J. G. Oh, J. Jung, S. H. Noh, T. S. Lee and J. Jang, *Adv. Energy Mater.*, 2020, **10**, 2002521.

8 P. Pingel, M. Arvind, L. Kölln, R. Steyrleuthner, F. Kraffert, J. Behrends, S. Janietz and D. Neher, *Adv. Electron. Mater.*, 2016, **2**, 1600204.

9 B. Yurash, D. X. Cao, V. V. Brus, D. Leifert, M. Wang, A. Dixon, M. Seifrid, A. E. Mansour, D. Lungwitz, T. Liu, P. J. Santiago, K. R. Graham, N. Koch, G. C. Bazan and T.-Q. Nguyen, *Nat. Mater.*, 2019, **18**, 1327–1334.

10 J. Lee, J. Kim, T. L. Nguyen, M. Kim, J. Park, Y. Lee, S. Hwang, Y.-W. Kwon, J. Kwak and H. Y. Woo, *Macromolecules*, 2018, **51**, 3360–3368.